

# Journal of Biomedical Optics

BiomedicalOptics.SPIEDigitalLibrary.org

## **Feasibility of quantitative diffuse reflectance spectroscopy for targeted measurement of renal ischemia during laparoscopic partial nephrectomy**

Utsav O. Goel  
Michael M. Maddox  
Katherine N. Elfer  
Philip J. Dorsey  
Mei Wang  
Ian Ross McCaslin  
J. Quincy Brown  
Benjamin R. Lee

# Feasibility of quantitative diffuse reflectance spectroscopy for targeted measurement of renal ischemia during laparoscopic partial nephrectomy

Utsav O. Goel,<sup>a</sup> Michael M. Maddox,<sup>a</sup> Katherine N. Elfer,<sup>b</sup> Philip J. Dorsey,<sup>a</sup> Mei Wang,<sup>b</sup> Ian Ross McCaslin,<sup>a</sup> J. Quincy Brown,<sup>b,\*</sup> and Benjamin R. Lee<sup>a</sup>

<sup>a</sup>Tulane University School of Medicine, Department of Urology, New Orleans, Louisiana 70112, United States

<sup>b</sup>Tulane University, Department of Biomedical Engineering, New Orleans, Louisiana 70118, United States

**Abstract.** Reduction of warm ischemia time during partial nephrectomy (PN) is critical to minimizing ischemic damage and improving postoperative kidney function, while maintaining tumor resection efficacy. Recently, methods for localizing the effects of warm ischemia to the region of the tumor via selective clamping of higher-order segmental artery branches have been shown to have superior outcomes compared with clamping the main renal artery. However, artery identification can prolong operative time and increase the blood loss and reduce the positive effects of selective ischemia. Quantitative diffuse reflectance spectroscopy (DRS) can provide a convenient, real-time means to aid in artery identification during laparoscopic PN. The feasibility of quantitative DRS for real-time longitudinal measurement of tissue perfusion and vascular oxygenation in laparoscopic nephrectomy was investigated *in vivo* in six Yorkshire swine kidneys ( $n =$  three animals). DRS allowed for rapid identification of ischemic areas after selective vessel occlusion. In addition, the rates of ischemia induction and recovery were compared for main renal artery versus tertiary segmental artery occlusion, and it was found that the tertiary segmental artery occlusion trends toward faster recovery after ischemia, which suggests a potential benefit of selective ischemia. Quantitative DRS could provide a convenient and fast tool for artery identification and evaluation of the depth, spatial extent, and duration of selective tissue ischemia in laparoscopic PN. © 2014 Society of Photo-Optical Instrumentation Engineers (SPIE) [DOI: 10.1117/1.JBO.19.10.107001]

Keywords: diffuse reflectance; spectroscopy; ischemia; kidney; laparoscopy; surgery.

Paper 140379R received Jun. 13, 2014; revised manuscript received Aug. 25, 2014; accepted for publication Sep. 16, 2014; published online Oct. 8, 2014.

## 1 Introduction

As the incidence of small renal masses increases, clinicians are seeking new ways to optimize the therapy by improving the technique and minimizing the harms of surgery, while focusing on a goal of maintaining oncologic efficacy. For this reason, partial nephrectomy (PN) was shown to have a number of advantages to radical nephrectomy, including its preservation of nephrons with equivalent oncologic control, even despite increased surgical complexity.<sup>1</sup> Indications for PN are increasing and generally fall into one of the several categories including: chronic kidney disease (CKD), solitary kidney, perihilar masses, endophytic tumors, bilateral tumors, and elective resection of tumors <4 cm or even <7 cm.<sup>1,2</sup> As robotic surgery evolves, new techniques will be developed in order to preserve as much renal tissue and function as possible.

Because robotic or laparoscopic surgery does not easily allow for cold ischemia of the renal tissue, the predominant method is to perform resection under warm ischemia, with inherent risks of renal injury with prolonged renal artery occlusion. Further refinements in PN are now focused on reducing blood loss, decreasing ischemia time, and improving renal function outcomes. Because open PN allows the surgeon to cool the renal parenchyma whereas laparoscopic/robotic PN does not, the warm ischemia time after clamping the renal artery is of paramount importance with respect to preservation of renal function. While many consider 30 min of warm ischemia the

“safe” threshold, recent studies indicate that every minute of hilar clamping may count.<sup>3,4</sup> Several studies have shown that the segmental or higher-order artery occlusion during PN affords superior functional outcomes.<sup>5,6</sup> These technical modifications, however, may extend operating time and increase the blood loss,<sup>7</sup> especially if artery identification is done imprecisely.

Due to studies showing that every minute of global warm ischemia counts toward renal function decline,<sup>8</sup> clinicians have adapted many different techniques to limit ischemia time; the evolution has progressed from total hilar clamping, to early unclamping, and finally to “zero-ischemia” (aka selective ischemia).<sup>9</sup> The zero-ischemia approach refers to eliminating global renal ischemia by microdissection and clamping of the higher-order segmental arteries feeding the tumor-containing area only, rather than clamping the primary renal artery supplying the entire kidney. In this way, nondiseased kidney tissue experiences no ischemia (“zero-ischemia”), whereas the tumor-containing region is devascularized so that it may be safely removed with minimal blood loss. Zero-ischemia, which theoretically preserves the glomerular filtration rate (GFR) for all nephrons outside the tumor watershed, has been shown to have significantly better postoperative functional results than global renal ischemia, regardless of surgical approach.<sup>10</sup> Renal function preservation is optimized with zero-ischemia PN whether via robotics<sup>11</sup> or laparoscopy<sup>12</sup> compared with a total hilar clamp control.

\*Address all correspondence to: J. Quincy Brown, E-mail: [jqbrown@tulane.edu](mailto:jqbrown@tulane.edu)

In the zero-ischemia method, the fundamental principle of “artery first, tumor second” requires imaging and localization methods to ensure that the correct higher order artery is occluded to ensure zero-ischemia.<sup>9</sup> In other words, before the tumor can be safely removed, the first step in the zero-ischemia technique is to identify the artery vascularizing the tumor-containing parenchyma and to ensure that the occlusion of that artery selectively devascularizes the tumor region, while maintaining adequate perfusion in the remainder of the kidney. Methods used to confirm selective ischemia have included color Doppler ultrasound imaging or intravenous indocyanine green (ICG) injection with infrared imaging to determine the tumor devascularization.<sup>9</sup> A pilot study of 34 patients demonstrated that the near-infrared fluorescence with ICG during robotic PN can characterize the renal vasculature in order to isolate the optimal artery for tumor ischemia.<sup>13</sup> However, neither of these methods reports specifically on vascular oxygenation, which is the endpoint of interest in the zero-ischemia method.

The spectral properties of hemoglobin (Hb) in response to binding of oxygen allow for quantitative diffuse reflectance spectroscopy (DRS) measurement of vascular Hb oxygen saturation ( $sO_2$ ) *in vivo*.<sup>14</sup> Spectroscopic tissue analysis has been used to monitor local changes in tissue  $sO_2$  and total Hb contents during periods of tissue ischemia.<sup>14,15</sup> A real-time spectroscopic measurement can confirm sufficient tumor ischemia<sup>16,17</sup> as well as reduce blood loss even in challenging tumor types.<sup>9</sup> This would allow surgeons to determine if the target artery perfusing the tumor has been identified, as well as to gauge the depth and spatial boundaries of ischemia. However, the feasibility of integrating quantitative DRS to quantify ischemia in real time during renal artery clamping has not yet been studied. In the present study, a fiber-optic-probe-based DRS system was used to longitudinally assess the local tissue oxygenation *in vivo* during normal perfusion, primary renal artery occlusion, and segmental (tertiary) renal artery occlusion, allowing a determination of the velocity with which ischemia is reached and the time to recovery following reperfusion. The feasibility of using fiber-optic optical spectroscopy for real-time measurement of renal ischemia during laparoscopic surgery is demonstrated in a large animal model, and preliminary results comparing time to ischemia and reperfusion in main versus segmental artery clamping are presented, as well as results demonstrating the utility of DRS for probing the depth and spatial boundaries of locally induced ischemia are presented.

## 2 Materials and Methods

Upon approval by the Institutional Animal Care and Use Committee, three Yorkshire swine (six kidneys) were allocated and prospectively underwent intraoperative *in vivo* spectroscopic tissue analysis using a Zenascope PC1 diffuse reflectance spectrometer (Zenalux Biomedical, Durham, North Carolina) during laparoscopic induction of either global or regional warm ischemia. The nonsurvival surgical procedures were supervised by veterinary personnel from the Tulane University IACUC.

The Zenascope PC1 spectrometer employs a broadband halogen light source to illuminate the target tissue. A bifurcated fiber optic probe with stainless steel jacketing and terminating in a 0.25-in diameter stainless steel rigid common end delivers light to the target tissue and collects the reflected optical signal, and the optical properties (wavelength-dependent absorption and scattering coefficients) of the tissue are quantitatively extracted

from the measured reflectance spectra over the wavelength range 500 to 650 nm, using a previously described inverse Monte Carlo (MC) model.<sup>18</sup> Briefly, optical properties (i.e., wavelength-dependent absorption and reduced scattering coefficient spectra) of the tissue under investigation are obtained by first generating a modeled diffuse reflectance spectrum for an initial set of optical properties, using a lookup table generated from a scaled MC simulation for the specific instrumentation and probe geometry used in the study. This modeled diffuse reflectance spectrum is compared with the calibrated diffuse reflectance spectrum measured from the unknown tissue, the input parameters are changed and the process repeated iteratively until the modeled and measured diffuse reflectance spectra are matched. At this point, the input optical properties (absorption and scattering coefficients) giving rise to the best match between the modeled and measured diffuse reflectance spectra are taken to be the optical properties of the unknown tissue sample. This fitting/inversion process is performed in about 0.5 s per spectrum on a low-end commodity laptop PC. The fiber-optic probe comprises a single 400- $\mu$ m illumination fiber and a single 400- $\mu$ m collection fiber, separated by 2-mm center-to-center. The separation distance of 2 mm offered a good balance between the reflectance signal and sensing depth. Using the modified MCML MC code developed by Liu et al.<sup>19</sup> and optical properties extracted from renal tissue in this study, the sensing depth of the probe for the wavelengths used in this study was found to range from 0.9 to 2 mm, depending on tissue optical properties. From the extracted absorption coefficient, the portable and standardized measurement hardware achieves rapid, real-time quantitative analysis of oxy-Hb ( $HbO_2$ ), deoxy-Hb (dHb), total Hb concentration (defined as  $HbO_2 + dHb$ ), and Hb oxygen saturation ( $sO_2$ , defined as the ratio  $HbO_2/Hb$ ). The optical reduced scattering coefficient ( $\mu'_s$ ) was also measured and reported by the instrument, which allows measurements of tissue chromophores to be quantified accurately and independently of changes in tissue scattering. Integration times were automatically set by the system software for each measurement to maximize reflectance signal, while staying within the linear response range of the detector, and typically ranged from 100 to 200 ms. Reflectance calibration of the probe using a 99% reflectance standard was performed prior to all experiments and periodically during the procedures.

Each animal subject underwent standard general anesthetic followed by insufflation with carbon dioxide to establish pneumoperitoneum. Three Laparoscopic trocars were placed and the renal capsule was exposed for each kidney followed by meticulous dissection of the hilar vasculature using standard laparoscopic techniques. The optical probe was inserted down one laparoscopic trocar and guided to the location of interest under endoscopic guidance. The probe was placed in gentle contact with the tissue (as assessed visually), and each kidney underwent both  $sO_2$  measurement and total Hb concentration measurement in multiple locations on the surface of the kidney. Figure 1 shows a screenshot of the endoscopic video feed showing the optical probe interfaced with the kidney during an intraoperative laparoscopic measurement. The endoscopy light source was turned off during spectroscopic measurements to prevent the contamination of the spectroscopic signal. The probe was placed onto the kidney surface using video guidance, ensuring that the probe was not placing pressure on the tissue by confirming that there was minimal deformation of the kidney surface (Fig. 1). To ensure that there were no effects of probe pressure on tissue physiology, several baseline

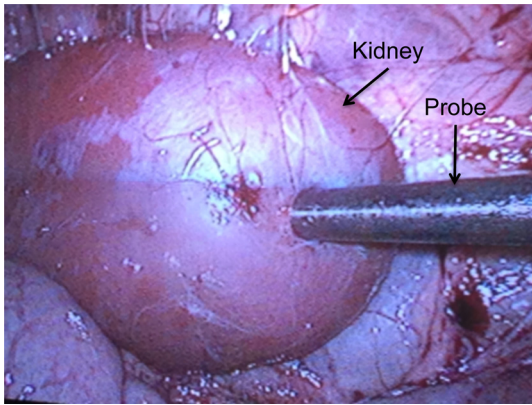


**Fig. 1** Screenshot of live video feed taken during intraoperative laparoscopic renal ischemia measurements. The optical probe was inserted through a 12-mm trocar and placed in contact with the desired location on the kidney using video endoscopy guidance.

measurements were made in the same location before starting each clamping challenge to ensure that they were repeatable. In four kidneys, the main renal artery was occluded using a laparoscopic bulldog clamp, while the remaining two kidneys underwent dissection and selective clamping of a tertiary segmental artery. To monitor the time course of ischemia and reperfusion, spectroscopic renal measurements were obtained at baseline (prior to clamping), approximately every 12 s during warm ischemia (approximately 2 to 5 min clamp duration) and every 12 s following reperfusion of the kidney. To determine the ability of the system to aid in artery identification, a segmental artery in the lower pole of the kidney was clamped, and spectra were acquired from multiple locations in the lower pole, the midpole, and the upper pole of the kidney, respectively. Spectra were analyzed in real time by the Zenascope software and endpoints were displayed on the computer screen; data were exported after the experiments for analysis in MATLAB and Microsoft Excel.

### 3 Results

Figures 2(a) and 2(b) contain calibrated reflectance spectra from normoxic ( $sO_2 = 82\%$ ) and ischemic ( $sO_2 = 0\%$ ) kidney tissue, respectively, along with the corresponding fits to the reflectance given by the inverse MC inversion algorithm. As observed in the figures, the inverse MC model provides excellent fits to the calibrated reflectance data. The troughs in the reflectance curve of Fig. 2(a) at 542 and 576 nm correspond to the  $\beta$  and  $\alpha$  absorption bands of oxygenated Hb, respectively, and are characteristic of tissues containing significant oxy-Hb content. Conversely, in the reflectance curve for ischemic kidney tissue in Fig. 2(b), these troughs are replaced by a single broad trough at 556 nm, corresponding to a significant contribution of deoxygenated Hb. From the inverse MC fit, the absorption coefficients of the tissues were extracted and are shown in Figs. 2(c) and 2(d). In order to compare the shape of the extracted absorption coefficients with expected Hb absorption curves, known absorption spectra for oxygenated and deoxygenated human Hb were normalized to their values at 500 nm and then linearly combined to obtain the expected absorption coefficients for  $sO_2 = 82\%$  [Fig. 2(c)] and  $sO_2 = 0\%$  [Fig. 2(d)]. Comparison of the calculated absorption coefficient spectra, with the absorption coefficient spectra extracted from reflectance of the tissue, shows

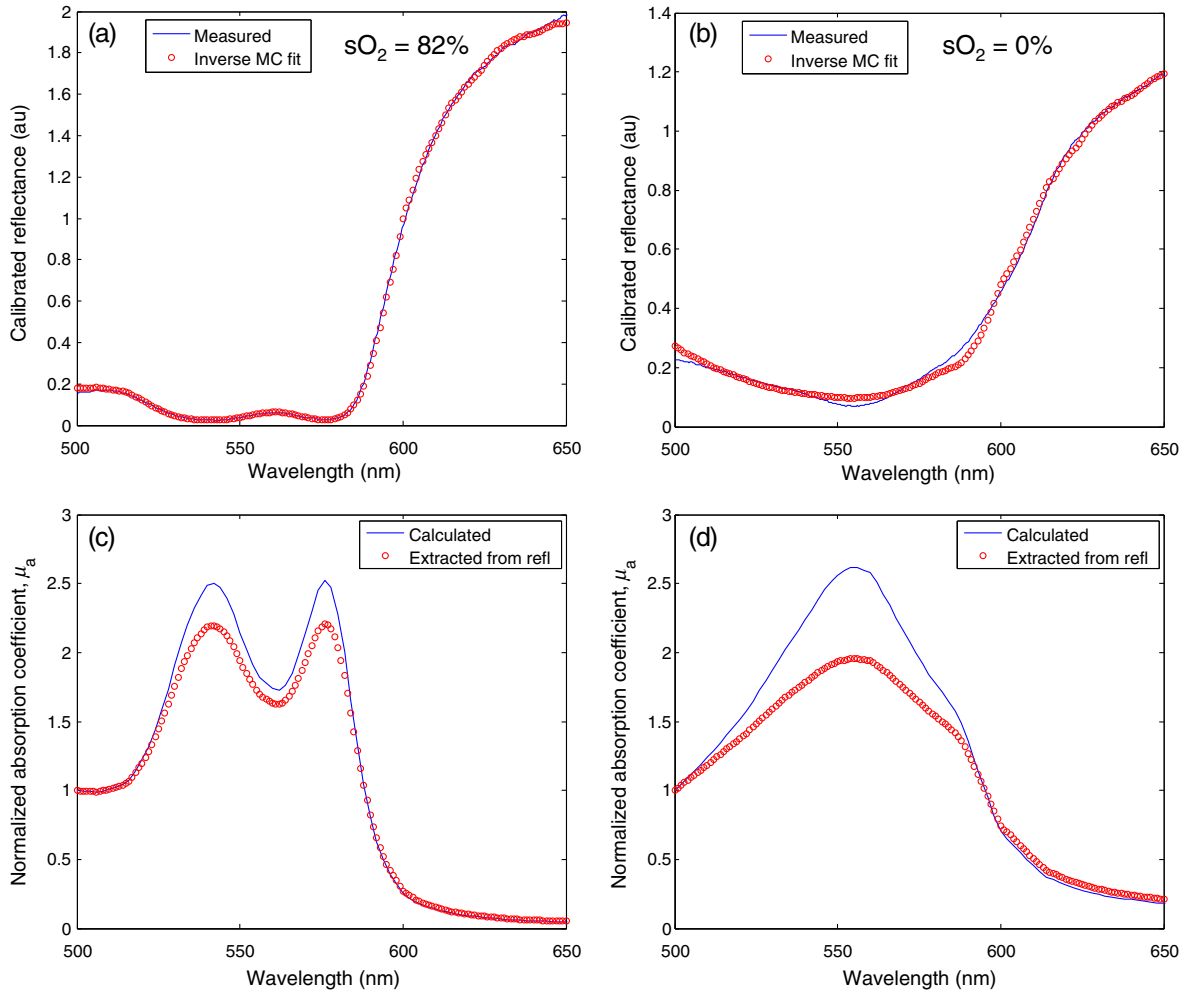
close agreement in spectral line shape, providing strong evidence for the validity of the extracted Hb saturation values.

Figure 3 demonstrates a typical time-course experiment with measurements of  $sO_2$  and Hb plotted against time in relation to clamping the primary renal artery. The mean time to ischemic steady state following clamping of the main renal artery was 22.3 s, with a range of 15 to 38 s. The mean time to recovery (time from unclamping at steady state until saturation reached maximal steady state) was 58.8 s with a range of 50 to 66 s. Inspection of the total Hb trace reveals reactive hyperemia following release of the renal artery, with the Hb concentration overshooting the initial preclamp value before returning to pre-clamp levels. The mean (wavelength averaged) reduced scattering coefficient was observed to be highly correlated with the Hb concentration, but not always in the same direction (for instance, the drop in scattering was negatively correlated with the spike in Hb concentration just after release of the clamp, but both scattering and Hb concentration were elevated compared with their respective clamped values, indicating a positive correlation).

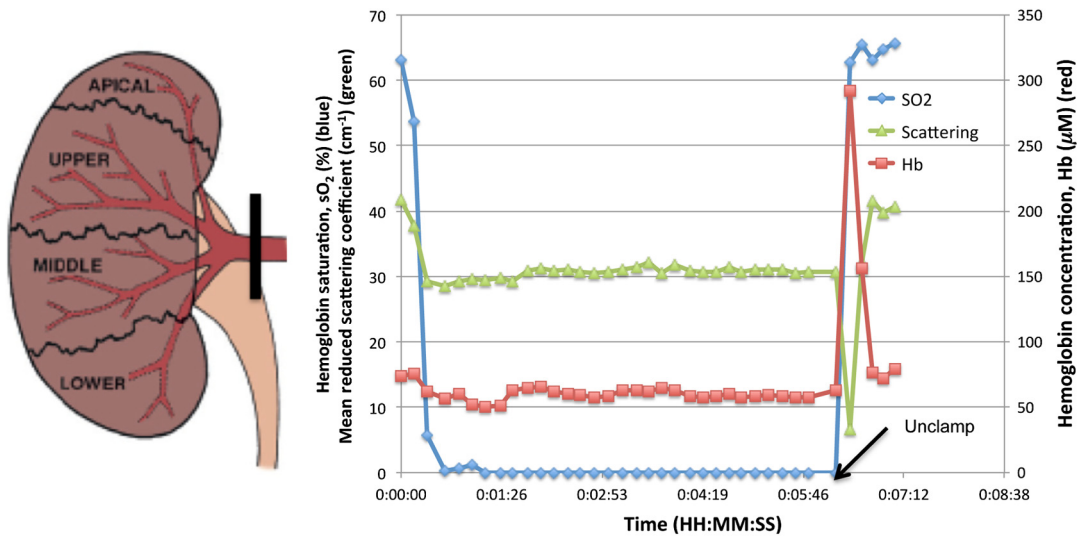
Figure 4 shows a typical time-course experiment for a tertiary artery occlusion trial. The mean time to ischemic steady state following clamping of the tertiary renal artery was 45.5 s (range 26 to 65). When compared with the kidneys following primary renal artery occlusion, the kidneys undergoing selective ischemia recovered more quickly, with a mean recovery time of 42.5 s (range 37 to 48). Interestingly, although reactive hyperemia following release of the primary renal artery was consistently observed, the same was not true for the tissues perfused by the tertiary arteries in the small sample set studied. Also, in this case the postdissection baseline, Hb saturation before and after clamping was overall lower than the predissection baseline, perhaps due to the effects of dissection.

Figure 5(a) summarizes the Hb saturation time course results for all six of the clamping trials grouped into the preclamp value (selected as the max  $sO_2$  just prior to clamping, but after dissection to expose the artery), the clamped value (min  $sO_2$  during clamping), and the released value (max  $sO_2$  after release of the clamp). The individual data points for each trial are shown in gray dots, the mean is shown as a horizontal red line, the red box indicates the 95% confidence interval, and the blue box indicates 1 standard deviation from the mean. The  $sO_2$  values in the clamped regime were significantly lower ( $p < 0.05$ ) than the preclamp and released values. However, the preclamp and released values were not significantly different from each other, indicating a stable return to baseline values after release of the clamp. Since each clamping experiment was taken over slightly different time scales and sampling frequencies, it was not possible to exactly overlay the time-course results for all time points on the same plot. Therefore, the same data from Fig. 5(a) are shown in Fig. 5(b) as three-point time-course curves, so that the  $sO_2$  behavior for each primary or tertiary clamping trial may be directly observed. Each trial resulted in a drop in  $sO_2$  during clamping, with return to baseline values after clamping. Table 1 demonstrates the differences in time to ischemia as well as recovery time between the two experimental models. The mean time to ischemia trended toward longer times with tertiary clamping, whereas the mean time to recovery trended toward shorter times with tertiary clamping.

Figure 6 shows the results of selective tertiary artery clamping in the lower pole of the kidney on vascular oxygenation in the lower, middle, and upper poles of the kidney. As expected, measurements taken proximally to the clamped



**Fig. 2** Measured calibrated reflectance curves and corresponding inverse Monte Carlo (MC) fits for (a) normoxic kidney with extracted  $sO_2 = 82\%$  and (b) ischemic kidney with extracted  $sO_2 = 0\%$ . Corresponding absorption coefficient spectra, extracted from the reflectance measurements of the tissues in (a) and (b), are shown in (c) and (d), respectively. Expected absorption coefficient spectra, calculated using the extracted  $sO_2$  measurements and the known absorption spectra of human oxy-Hb and deoxy-Hb, are shown in (c) and (d) for comparison.



**Fig. 3** Representative time series measurement of Hb saturation ( $sO_2$ , blue curve) and total Hb concentration (Hb, red curve) in response to clamping of the primary renal artery (shown diagrammatically at left). The time course begins at the time of clamping (00:00:00); the time point at which the clamp was released is indicated in the plot.

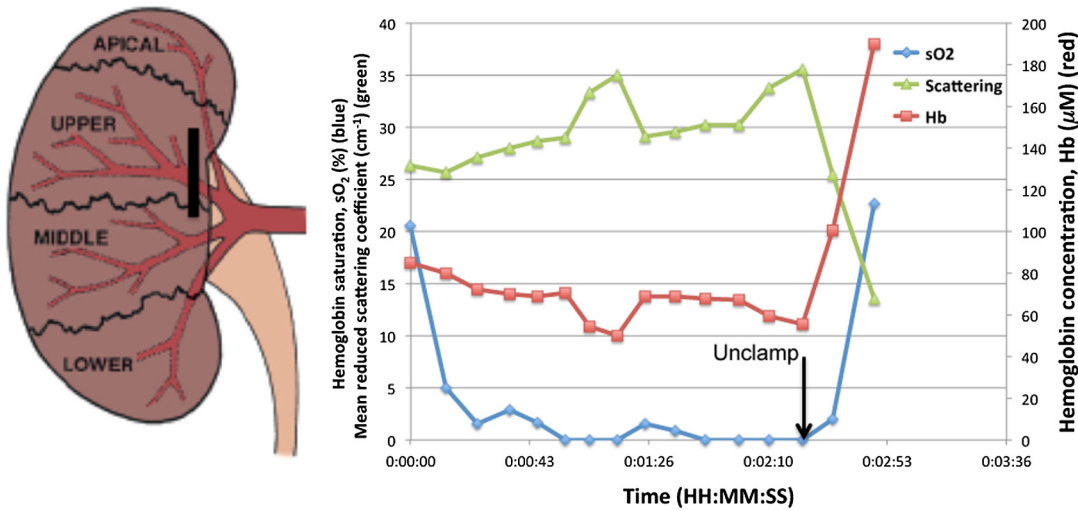


**Fig. 4** Representative time series measurement of Hb saturation ( $sO_2$ , blue curve) and total Hb concentration (Hb, red curve) in response to clamping of an upper tertiary segmental artery (shown diagrammatically at left). The time course begins at the time of clamping (00:00:00); the time point at which the clamp was released is indicated in the plot.

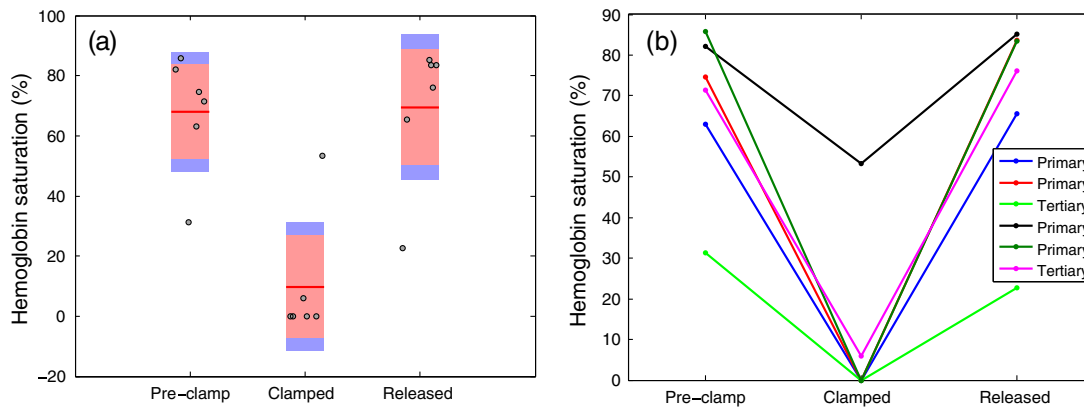


**Fig. 5** Hb saturation values for all six time course trials, corresponding to the preclamp regime (max  $sO_2$  prior to clamping), clamped regime (min  $sO_2$  after clamping), and released regime (max  $sO_2$  after release of the clamp). (a) Individual data points for each time regime are shown as gray dots. The horizontal red line corresponds to the mean, the red box corresponds to the 95% confidence interval, and the blue box corresponds to 1 standard deviation. (b) Three-point time course curves are shown for each trial (indicated as primary or tertiary clamping in the figure legend).

**Table 1** Mean time to ischemia and mean time to recovery for the six kidneys examined in this work, for primary renal artery (4) versus tertiary segmental branch (2) clamping.

	Primary clamping	Tertiary clamping
Mean time to ischemia (10% max "pre" $sO_2$ ) (s) (range)	22.3 ± 10.8 (15 to 38)	45.5 ± 27.6 (26 to 65)
Mean time to recovery (90% max "post" $sO_2$ ) (s) (range)	58.8 ± 6.6 (50 to 66)	42.5 ± 7.8 (37 to 48)

renal segment were more poorly oxygenated and spatially heterogeneous (mean ± standard deviation = 21 ± 3.3%  $sO_2$ ), compared with the measurements taken from the opposite (upper) pole of the kidney (mean ± standard deviation = 75 ± 1.2%  $sO_2$ ). Measurements taken from the middle pole of the kidney exhibited an intermediate oxygenation

(mean ± standard deviation = 33 ± 1.9%  $sO_2$ ). All postclamp  $sO_2$  measurements were lower than the preclamp, predissection baseline, perhaps due to blood loss effects during dissection.

### 4 Discussion

The question of comparing selective tertiary artery clamping with total renal artery occlusion is important in minimizing post-operative renal function decline. With CKD prevalence increasing in the patient population, any intervention supporting renal function must be explored. Complications such as increased hospital stays, cardiac events, and even death have all been attributed to compromised renal function.<sup>20</sup> Outcomes for super selective artery occlusions have been shown to be better than or at least equivalent to total hilar clamping in relation to many different metrics.<sup>11</sup> Most studies focus on three areas of comparison: immediate and long-term GFR preservation, oncologic control in terms of margin status and recurrence, and complications with special attention to bleeding and operative times.

Quantitative DRS may represent a simpler, more direct, and more cost-effective system to be used in the future of the zero-ischemia technique than previously investigated methods. While this study is the first to show the feasibility of quantitative DRS in renal porcine models laparoscopically, tissue oximetry and spectroscopy measurements have been shown to be efficacious in assessing renal function and local tissue ischemia in open nephrectomy.<sup>13,21</sup> In renal tissue specifically, investigators have previously shown with hyperspectral imaging during open nephrectomy that the tissue oxygenation is heterogeneous in opposing poles of the kidney even when the primary artery is occluded.<sup>22</sup> Another spectral imaging study demonstrated the evidence of heterogeneous ischemia due to main renal artery clamping.<sup>23</sup> Quantitative DRS during PN as demonstrated in this work focuses on using the probe in real time in various locations around the tumor to determine if ischemia is adequate and selective. Our study is the first to our knowledge to use a spectroscopic technique to monitor ischemia in real time due to clamping of the main renal artery versus clamping of tertiary segmental arteries. Our results in this laparoscopic porcine model indicate a slower recovery from ischemia when the main renal artery was occluded compared with a tertiary artery. This is potentially significant given the need to reduce warm ischemia time in laparoscopic or robotic PN. The segmental artery occlusion showed slower time to ischemia and faster recovery time. Because the main renal artery was not occluded but rather only a tertiary branch, one possible explanation of our findings is the preservation of venous circulation causing a pressure buildup and backflow from the other kidneys. While we were not able to obtain enough samples for tertiary clamping to test for statistical significance of these ischemia and recovery response time results, our observations nonetheless are consistent with current qualitative understanding and suggest a potential use for the device in future studies aiming at quantifying these effects.

These data were easily reproducible and consistent across all kidneys, as demonstrated in Fig. 5. Given the utility and ease-of-use of the tissue spectrometer used in this work, these measurements can be standardized and used in real time during surgery. For the time-course experiments,  $sO_2$  nadir values during clamping were low (between 0% and 10%), except for one primary artery trial, where the  $sO_2$  nadir during clamping was 53%. We believe that in this case we unwittingly placed the probe at the boundary of the devascularized region—this speculation is supported by the results of Fig. 6, where we found that the selective clamping of a tertiary artery in the lower pole of the kidney resulted in a gradient of oxygenation, from poorly perfused in the ipsilateral (lower) pole, to moderately perfused in the mid-pole, to well-perfused in the contralateral (upper) pole. We observed that the clamping of a tertiary artery in one pole decreased the Hb saturation of the opposite pole (Fig. 6), although to a lesser extent than locally to the clamped artery. We also noted that the vascular oxygenation measurements of the perfused kidney were lower after dissection and clamping compared with baseline measurements taken before dissection of the kidney. This suggests that quantitative DRS could be used to determine whether lasting effects of surgery on perfusion in the remaining kidney are present, which could have implications for prognosis related to postoperative kidney function in the zero-ischemia technique. Although, due to our limited sample size, we can draw no definitive statistical conclusions about the spatial extent of ischemia due to segmental artery clamping, these data demonstrate the utility of a real-time system for

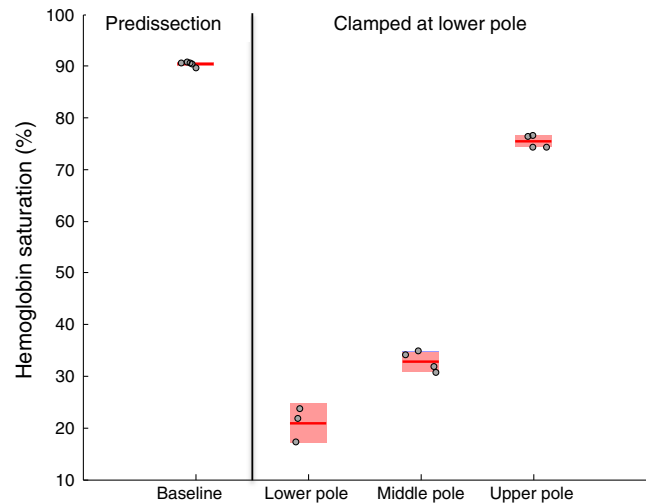


**Fig. 6** Hb saturation at baseline (predissection and preclamp,  $n =$  five locations) and at the lower ( $n = 3$ ), middle ( $n = 4$ ), and upper ( $n = 4$ ) poles of the kidney after dissection and clamping of a tertiary artery in the lower pole (postclamp). Individual data points for each pole location are shown as gray dots. The horizontal red line corresponds to the mean, the red box corresponds to the 95% confidence interval, and the blue box corresponds to 1 standard deviation.

assessing the same, which could be useful in identification of arteries afferent to the tumor region, for delineating the depth of ischemia, and for mapping the areas of the tissue rendered ischemic by clamping, as demonstrated in Fig. 5.

One advantage of the device used here, in comparison with noncontact hyperspectral imaging systems, is that it provides a real-time quantitative measurement of tissue absorption and scattering coefficients independently of each other with minimal calibration and complexity. This is enabled by the contact probe, which provides well-defined illumination and collection geometries at the tissue surface, combined with the inverse MC optical property extraction algorithm. A disadvantage compared with imaging systems is that it is limited to point measurements; however, the speed of the measurement and simplicity of interpretation could still provide an attractive and useful tool for quickly “spot checking” devascularization during selective ischemia. Although in this study we focus primarily on parameters related to tissue absorption, namely Hb concentration and  $sO_2$ , the tissue scattering coefficient was also determined and was found to be correlated with the Hb concentration during the time course clamping trials, although not in consistent directions. We do not currently have a hypothesis as to the mechanism behind these observations. However, we note that the ability to measure scattering independent of ischemia measurements could provide additional information, for instance serving as an aid in distinguishing tumor tissue from normal tissue prior to induction of ischemia during PN.<sup>14,24</sup> This will be the subject of future study.

One limitation of this nonsurvival study is the lack of correlation of our intraoperative findings to postoperative measures of renal function. Another limitation was that this methodology was not extended for PNs, and measures such as blood loss, transfusion rates, or operative times were not compared. Finally, our study is further limited by the small number of subjects and, thus, serves primarily as a feasibility study. However, we have demonstrated that the use of quantitative DRS may be a cost effective and logistically uncomplicated tool to assess

adequate ischemia with selective arterial clamping during PN. In addition, our results indicate a quicker recovery from ischemia with selective arterial clamping, which may partially explain the mechanism behind renal function preservation with selective clamping compared with total hilar clamping. It is important to note that the vascular Hb sO<sub>2</sub> results reported here are for warm ischemia at physiological temperatures. The use of this (or similar) technology for measurement of vascular oxygenation in cold ischemia would require additional care in interpretation, due to the substantial increase in the Hb oxygen binding affinity with decreasing temperature.<sup>25</sup> We plan to investigate further the use of quantitative DRS during PN with correlation to postoperative renal function outcomes.

## 5 Conclusion

Quantitative VIS-NIR DRS is a useful and noninvasive method with which clamping status, segmental ischemia confirmation, and recovery from ischemia can be assessed in real time. Warm ischemia time may ultimately be reduced with the use of DRS to guide implementation of selective ischemia via hilar dissection and higher-order artery clamping. Further study is necessary in order to validate DRS-assisted ischemia and recovery velocities as predictors of postoperative renal function as well as logistically optimizing DRS for robotic or laparoscopic PN platforms.

## Acknowledgments

This work was supported in part by a grant from the Tulane University Provost's Fund (JQB). KNE acknowledges support from the National Science Foundation Graduate Fellowship.

Disclosures: JQB has financial interest in and has previously served as an employee or consultant of Zenalux Biomedical, Inc., which manufactures the optical spectrometer used in this work. Zenalux Biomedical, Inc. did not fund the present study, either in cash or in kind, and was not involved in its direction, execution, or interpretation.

## References

- E. Kheterpal and S. S. Taneja, "Partial nephrectomy: contemporary outcomes, candidate selection, and surgical approach," *Urol. Clin. North Am.* **39**(2), 199–210 (2012).
- A. A. Caire et al., "Near-infrared tissue oximetry and digital image analysis: quantification of renal ischaemia in real time during partial nephrectomy," *BJU Int.* **109**(2), 311–315 (2012).
- A. R. Patel and S. E. Eggener, "Warm ischemia less than 30 minutes is not necessarily safe during partial nephrectomy: every minute matters," *Urol. Oncol.* **29**(6), 826–828 (2011).
- R. H. Thompson et al., "Every minute counts when the renal hilum is clamped during partial nephrectomy," *Eur. Urol.* **58**(3), 340–345 (2010).
- B. M. Benway et al., "Selective versus nonselective arterial clamping during laparoscopic partial nephrectomy: impact upon renal function in the setting of a solitary kidney in a porcine model," *J. Endourol.* **23**(7), 1127–1133 (2009).
- N. J. Harty et al., "Temporary targeted renal blood flow interruption using a reverse thermosensitive polymer to facilitate bloodless partial nephrectomy: a swine survival study," *BJU Int.* **110**(6 Pt B), 274–280 (2012).
- P. Shao et al., "Laparoscopic partial nephrectomy with segmental renal artery clamping: technique and clinical outcomes," *Eur. Urol.* **59**(5), 849–855 (2011).
- A. R. Patel and S. E. Eggener, "Warm ischemia less than 30 minutes is not necessarily safe during partial nephrectomy: every minute matters," *Urol. Oncol.* **29**(6), 826–828 (2011).
- I. S. Gill et al., "Zero ischemia anatomical partial nephrectomy: a novel approach," *J. Urol.* **187**(3), 807–814 (2012).
- G. Simone et al., "Zero-ischemia minimally invasive partial nephrectomy," *Curr. Urol. Rep.* **14**(5), 465–470 (2013).
- M. M. Desai et al., "Robotic partial nephrectomy with superselective versus main artery clamping: a retrospective comparison," *Eur. Urol.* **66**(4), 713–719 (2014).
- A. K. George et al., "Perioperative outcomes of off-clamp vs complete hilar control laparoscopic partial nephrectomy," *BJU Int.* **111**(4 Pt B), E235–E241 (2013).
- M. S. Borofsky et al., "Near-infrared fluorescence imaging to facilitate super-selective arterial clamping during zero-ischaemia robotic partial nephrectomy," *BJU Int.* **111**(4), 604–610 (2013).
- J. Q. Brown et al., "Advances in quantitative UV-visible spectroscopy for clinical and pre-clinical application in cancer," *Curr. Opin. Biotechnol.* **20**(1), 119–131 (2009).
- J. A. Wahr et al., "Near-infrared spectroscopy: theory and applications," *J. Cardiothorac. Vasc. Anesth.* **10**(3), 406–418 (1996).
- S. L. Best et al., "Renal oxygenation measurement during partial nephrectomy using hyperspectral imaging may predict acute postoperative renal function," *J. Endourol.* **27**(8), 1037–1040 (2013).
- J. Q. Brown et al., "Quantitative optical spectroscopy: a robust tool for direct measurement of breast cancer vascular oxygenation and total hemoglobin content in vivo," *Cancer Res.* **69**(7), 2919–2126 (2009).
- G. M. Palmer and N. Ramanujam, "A Monte Carlo-based inverse model for calculating tissue optical properties. Part I: theory and validation on synthetic phantoms," *Appl. Opt.* **45**(5), 1062–1071 (2006).
- Q. Liu, C. Zhu, and N. Ramanujam, "Experimental validation of Monte Carlo modeling of fluorescence in tissues in the UV-visible spectrum," *J. Biomed. Opt.* **8**(2), 223–236 (2003).
- A. S. Go et al., "Chronic kidney disease and the risks of death, cardiovascular events, and hospitalization," *N. Engl. J. Med.* **351**(13), 1296–1305 (2004).
- N. J. Crane et al., "Visual enhancement of laparoscopic partial nephrectomy with 3-charge coupled device camera: assessing intraoperative tissue perfusion and vascular anatomy by visible hemoglobin spectral response," *J. Urol.* **184**(4), 1279–1285 (2010).
- J. D. Raman et al., "Comparison of tissue oxygenation profiles using 3 different methods of vascular control during porcine partial nephrectomy," *Urology* **74**(4), 926–931 (2009).
- N. J. Crane et al., "Evidence of a heterogeneous tissue oxygenation: renal ischemia/reperfusion injury in a large animal model," *J. Biomed. Opt.* **18**(3), 035001 (2013).
- J. P. Couapel et al., "Optical spectroscopy techniques can accurately distinguish benign and malignant renal tumours," *BJU Int.* **111**(6), 865–871 (2013).
- R. K. Dash and J. B. Bassingthwaite, "Blood HbO<sub>2</sub> and HbCO<sub>2</sub> dissociation curves at varied O<sub>2</sub>, CO<sub>2</sub>, pH, 2,3-DPG and temperature levels (vol 32, pg 1676, 2004)," *Ann. Biomed. Eng.* **38**(4), 1683–1701 (2010).

**Utsav O. Goel** is a medical student at Tulane School of Medicine with anticipated graduation in 2015. He completed his undergraduate studies from Northwestern University, Evanston, IL, in 2011, with a BA degree in linguistics and cognitive science. He is currently serving on the Board of Governors of the Louisiana State Medical Society and is a delegate on behalf of the medical student section to the American Medical Association House of Delegates.

**Michael M. Maddox** is a clinical instructor and endourology fellow at Tulane University School of Medicine and Medical Center. He graduated from the University of Tennessee in 2004. He then completed medical school at the University of Tennessee Health Science Center in 2008. After medical school, he completed his general surgery internship and urology residency at Brown University/Rhode Island Hospital in 2013. He is an active member of the American Urologic Association.

**Katherine N. Elfer** is a third-year PhD student in biomedical engineering at Tulane University. She completed her BS degree in nanosystems engineering at Louisiana Tech University, and currently she is a National Science Foundation Graduate Research Fellow. She was raised in the Greater New Orleans area and continues to be involved in local outreach programs for fostering scientific exploration in K-12 students.

**Philip J. Dorsey** completed his urology residency at the Tulane University School of Medicine in July 2014 and is now a clinical urologist in private practice in south New Jersey. He graduated from Vanderbilt University in 2004 and completed medical school at Tulane in 2008. After medical school, he returned to Tulane for his internship and urology residency training. He is an active member of the American Urologic Society.

**Mei Wang** received her BS degree in biomedical engineering in 2012 and her MS degree in biomedical engineering in 2013, both from Tulane University. She is currently a PhD candidate in the Department of Biomedical Engineering, Tulane University.

**Ian Ross McCaslin** is a urology resident at Tulane University School of Medicine. He graduated from the University of California, Davis, in 2007. He then completed medical school at Tulane University School of Medicine in 2013. After medical school, he remained at Tulane for his general surgery internship and urology residency training.

**J. Quincy Brown** is the Paul H. and Donna D. Flower assistant professor of engineering at Tulane University and the director of the Translational Biophotonics Laboratory. He received the BS degree in biomedical engineering in 2001, and the PhD degree in 2005, both from Louisiana Tech University. He joined the faculty of Tulane University in 2012, following postdoctoral training at Duke University. He is a member of SPIE, OSA, BMES, and IEEE EMBS.

**Benjamin R. Lee** is a professor of urology and oncology at the Tulane University School of Medicine. He obtained the BS degree from Cornell University and the MD degree from Johns Hopkins School of Medicine, continuing at Johns Hopkins for residency in urology. He was promoted to professor with tenure in the Department of Urology at Tulane in 2008 and was awarded the prestigious Arthur Smith Award in 2008 for his contributions to the discipline of robotics, laparoscopy, and minimally invasive surgery.